HHS Public Access

Author manuscript

Abdom Radiol (NY). Author manuscript; available in PMC 2017 June 05.

Published in final edited form as:

Abdom Radiol (NY). 2016 May ; 41(5): 854–861. doi:10.1007/s00261-016-0646-6.

The expanding landscape of diffusion-weighted MRI in prostate cancer

Andreas Wibmer, MD, **Evis Sala, MD, PhD**, **Hedvig Hricak, MD, PhD**, and **Hebert Alberto Vargas, MD**

Memorial Sloan Kettering Cancer Center; Department of Radiology. 1275 York Avenue, New York, NY, USA 10021

Abstract

The added value of diffusion-weighted magnetic resonance imaging (DW-MRI) for the detection, localization, and staging of primary prostate cancer has been extensively reported in original studies and meta-analyses. More recently, DW-MRI and related techniques have been used to non-invasively assess prostate cancer aggressiveness and estimate its biological behavior. The present article aims to summarize the potential applications of DW-MRI for non-invasive optimization of pretherapeutic risk assessment, patient management decisions, and evaluation of treatment response.

Introduction

More than thirty years have passed since the first in-vivo magnetic resonance imaging (MRI) studies of the prostate. The anatomical MRI sequences (T1- and T2-weighted) applied in the early day of MRI remain valid and represent the workhorses of prostate MRI, but currently these are supplemented with a multiparametric approach which includes one or more 'functional' imaging sequences, including diffusion-weighted (DW), dynamic contrast-enhanced (DCE), and/or MR-spectroscopy (MRS) techniques [1–2]. The last decade has witnessed mounting research activities on these techniques, particularly on DW-MRI, as reflected in the increasing number of Medline entries on this topic for the assessment of prostate cancer (Figure 1).

Extensive literature is now available that documents that the addition of DWI to standard T2w sequences significantly improves the diagnostic performance of prostate MRI [3–5]. A recently published meta-analysis concluded that a two-parameter approach (i.e. T2w MRI + DWI *or* DCE) may be sufficient for routine prostate imaging and that the combination of T2w MRI plus DWI may be more favorable [6]. Emerging high-resolution techniques might further increase the sensitivity of DWI to small or sparse cancer foci despite their lower signal-to-noise and contrast-to-noise ratios [7–8]. At present, as a broad body of evidence supports the routine application of DW-MRI from a diagnostic accuracy perspective, the scientific interest has expanded towards possible clinical implications of DWI-derived

Corresponding author: HA Vargas MD, 1275 York Av, Room C278, New York, NY 10065, vargasah@mskcc.org, Phone: (+1) 212-639-4017, Fax: (+1) 212-794-4010.

parameters and their decision-support potential. There are a growing number of publications documenting potential applications of DWI for non-invasive optimization of pre-therapeutic risk assessment, patient management decisions, and evaluation of treatment response. In this review, we aim to provide current state and scientific trends in these fields.

DW-MRI as a tool for risk-assessment

The well recognized biological heterogeneity of PCa is considered the key factor influencing the exceptionally variable natural history of the disease. A considerable proportion of slow-growing, indolent cancers do not affect the patients' life expectancy, as repeatedly shown in the literature and recently summarized in a meta-analysis of autopsy-studies from the prostate-specific antigen (PSA) era that reported a 47.3% prevalence of undiagnosed PCa in men aged 80 or older [9]. Other patients, however, suffer from rapidly expanding, metastatic and often fatal clones [10]. At the time of diagnosis, accurate risk-assessment is therefore crucial to avoid potentially harmful overtreatment for the former and delayed treatment for the latter group. The pathologic Gleason scoring (GS) system and its 2005 revised version [11] build the basis for the vast majority of currently applied risk-assessment tools. A recent analysis from the John's Hopkins Hospital confirmed the prognostic significance of the GS in a modern series of 7,869 patients and proposed a 5-point prognostic scale (i.e. grade I: GS 3+3=6; grade II: GS 3+4=7; grade III: GS 4+3=7; grade IV: GS 4+4=8; grade V: GS ≥9) [12]. The challenge with the GS, however, is that there are considerable discrepancies between GS on transrectal ultrasound (TRUS) biopsy-derived and prostatectomy-derived histological specimen. A meta-analysis of 14,839 patients showed that after radical prostatectomy, 38% of all GS 2–6 tumors were upgraded and 50% of GS 8–10 tumors were downgraded [13]. On this issue, DW-MRI may offer two types of problem-solving strategies, i.e. (1) generation of quantitative parameters for GS-estimation and (2) selection of an appropriate target lesion for guided biopsy.

It was in the late 2000's that researchers noticed that the degree of diffusion restriction of PCa foci, as quantified by the apparent diffusion coefficient (ADC), correlates with the lesion's GS on whole-mount histopathology specimen [14–21]. It has also been demonstrated that the median ADC value of a MRI-visible focus is a better predictor of the presence of intermediate- or high-risk PCa (i.e. GS>6 on prostatectomy specimen) than TRUS-guided biopsy [22]. Subsequent research revealed that histogram-derived descriptive variables, such as the 10^{th} percentile of the ADC, may perform better in predicting the final GS than the lesion's mean/median ADC [23–24]. However, the overlap of ADC values for different GS was substantial in these studies, meaning that there was no clear cut-off ADC-value for the distinction of low- vs. high-grade cancers (Figure 2).

This variability of ADC-values might be explained by biological as well as technical considerations. On a micro-anatomical level, the median ADC was shown to correlate with the cell density and amount of glandular tissue within a single 2.5×2.5 mm^2 voxel but not consistently with the prevalent Gleason pattern [25]. Others verified that cell density of a PCa lesion is a major determinant of its pixel-by-pixel ADC-value [26], and that its ADC-value is also influenced by the proliferation rate, as assessed by its Ki-67 labeling index [27]. The fact that the extent of diffusion restriction is not exclusively determined by the

Gleason pattern but other additional biological features may explain the repeatedly observed imperfect correlation between ADC and GS. Technical issues complicate matters. Although ADC-measurements are well reproducible on an intra-individual level [28], they are highly dependent on technical factors, e.g. the choice of b-values [29–30] or the use of an endorectal coil [31]. One approach to overcome the inherent problem of reproducibility and comparability of ADC-measurements is to analyze the spatial relation of single voxels within a tumor rather than statistical descriptors of absolute whole-lesion ADC-values. Texture analysis, for example, is one way to mathematically describe the degree of disorder among the voxels within a tumor, as schematically demonstrated in Figure 3 and Figure 4.

This method was shown to deliver ADC-map derived parameters that are independently associated with a lesion's GS [32] and outperformed mean ADC in estimating the amount of Gleason 4 pattern in GS 7 tumors [33]. Another approach to overcome the limitations of conventional DW-MRI is the application of more advanced DWI-techniques, such as diffusion kurtosis imaging or intravoxel incoherent motion imaging [34]. Intravoxel incoherent motion (IVIM) imaging is a DWI-technique that uses three or more b-values in order to account for the non-monoexponential behavior of ADC as a function of b-values. It also allows to separate true diffusion effects from perfusion (i.e. 'pseudo-diffusion') effects at low b-values. In prostate cancer, IVIM-derived variables (i.e. molecular diffusion coefficient D, and perfusion fraction f) were shown to be significantly lower than in benign prostate tissue [35–36]. Others found that high-grade prostate cancers had significantly lower D-values than low-grade lesion, allowing for a more accurate estimation of tumor grade than ADC [37]. In another analysis, however, f and the perfusion-related diffusion coefficient (D*) were not significantly different in prostate cancer and benign prostatic hyperplasia [36] and further research will have to identify the true clinical value of this novel technique. Diffusion kurtosis imaging (DKI) is a DWI-technique that takes into account that water molecules in biological tissues do not follow a Gaussian pattern of distribution. This deviation from a uniform diffusion pattern can be mathematically described as kurtosis and visualized by DKI, which applies diffusion gradients with multiple b-values in multiple spatial directions [38]. The DKI-derived metric K has been shown to be significantly different in cancer than in non-cancerous prostate tissue [39] and has also been used to differentiate high-grade from low-grade prostate cancer [40–42]. Others, however, found that the K-values of prostate cancer and benign prostatic hyperplasia showed marked overlap [43] and that DKI-derived metrics did not provide a significant benefit for detection and grading of prostate cancer when compared to standard ADC-maps [44]. An excellent review on the basic principles and body-imaging applications of DKI is provided in [45].

In contrast to standard TRUS-guided biopsy, where tissue samples are taken in a systematic fashion from pre-defined regions of the prostate gland, DW-MRI targets the lesion with the highest restriction on ADC maps (i.e. the 'index lesion'). With this approach, Hambrock and colleagues were able to correctly determine the highest Gleason grade in 88% of patients prior to prostatectomy (n=34), compared to 55% of a matched control group (n=64) who underwent TRUS-guided biopsy (p=0.001) [46]. Zhang et al. directly compared the two methods in a single cohort of 48 patients prior to radical prostatectomy [47] and found that DW-MRI guided biopsy correctly assessed the highest Gleason grade in 77.1 % vs. 72.9% for TRUS-guided biopsy (p=0.727). The different outcomes of these two prospective studies

might be explained by the different techniques applied for DW-MRI guided biopsy, each with different strengths and limitations. While Hambrock and colleagues biopsied the patients within the MR scanner (i.e. in-bore approach), Zhang et al. performed fusion biopsies, a technique that fuses stored MR-images with real-time ultrasound. A prospective trial in 54 patients with low-risk prostate cancer who underwent MR-guided biopsy of cancer-suspicious lesions showed that the mean ADC accurately predicted the presence and grade of PCa in these lesions (area under the ROC-curve for the presence of PCa: 0.73) [48]. DW-MRI guided biopsy may therefore increase the accuracy of pre-therapeutic risk assessment but further studies are needed to resolve technical issues and definitively prove its superiority to standard biopsy strategies.

DW-MRI as a support for management decisions

Due to the significant biological heterogeneity of PCa and the relatively indolent nature of a considerable proportion of cancers, active surveillance (AS) is becoming an accepted alternative management approach to radical treatment in patients with localized low-risk PCa. A nationwide survey among 2,133 Japanese urologists in January 2014, for instance, revealed that 73.1% of them used some sort of AS, although the authors found a substantial variation of inclusion criteria and follow-up protocols [49]. There is a growing body of literature verifying that AS is a reasonable and safe management strategy for selected PCa patients. In a recent report on a series of 469 men being managed by AS between 1997 and 2009, the 10-year cancer specific survival rate was 100% [50]. However, about a quarter of this cohort dropped out of the AS-protocol, most commonly due to pathologic progression on re-biopsy, PSA-progression, and patient preference, and the estimated probability of undergoing treatment within 10 years after the start of AS was reported to be 38% [50]. Given this considerable drop-out rate, there is the need for more reliable risk-assessment tools that can substantiate the decision of AS eligibility. There are some encouraging reports in the literature pointing towards DW-MRI-derived parameters, most importantly ADC, being a step in this direction. In a prospective study of 86 men managed by AS for low-risk PCa, tumor ADC was a significant predictor of upgrading on repeat biopsy and deferred radical treatment (incidence: 45%, area under the AUC curve: 0.83) [51]. These findings were reaffirmed by other studies that found that a lesion’s mean ADC or semi-quantitatively assessed degree of diffusion restriction on ADC maps were independent predictors of disease progression, upgrade on repeat biopsy, and/or switch to radical treatment [52–54]. In a prospective study on 50 men on AS showed that patients who progressed to radical treatment showed a significant drop of tumor mean ADC on follow-up DW-MRI while mean ADC remained stable in non-progressors [55]. Tumor volume on ADC maps might be another parameter that could optimize patient selection for AS, as shown in a group of 188 candidates for AS, in whom the tumor lesion’s diameter was an independent predictor of insignificant PCa (odds ratio: 0.32, p=0.014) [56]. More advanced DW-MRI techniques, such as diffusional kurtosis imaging [57] or diffusion-prepared balanced steady-state free precession [8] are possible alternatives to ADC values, and preliminary data shows that in candidates for AS they may predict unfavorable histology more accurately [57,8]. DW-MRI may also be useful to identify patients who get overgraded on TRUS-guided prostate biopsy and are incorrectly deemed nonsuitable for AS. In a study of 304 patients who had been

diagnosed with a GS 3+4=7 cancer on TRUS-guided biopsy, Gondo et al. identified T2- and DW-MRI-derived information as independent predictors of a GS 3+3=6 on final prostatectomy-derived histopathology (area under the ROC curve: 0.88–0.92). Their MRI-based predictive model outperformed a model solely based on clinical parameters (area under the ROC curve: 0.73). For patients after radical prostatectomy, the ADC value of the index lesion was shown to be an independent predictor of biochemical recurrence [58].

Focal ablation therapies, such as high-intensity focused ultrasound (HIFU), cryo- or laser-ablation, are emerging alternatives to radical treatment in localized PCa. It is hoped that these techniques may achieve local tumor control with preservation of erectile and urinary function. Similar to AS, proper patient selection is crucial for successful implementation of these minimal-invasive treatment strategies. DW-MRI may support selection algorithms and definition of target areas within the gland, as demonstrated in some preliminary studies. In their study on 162 candidates for focal PCa therapy, Matsuoka and colleagues showed that with the addition of DW-MRI to 14-core TRUS-guided biopsy, the negative predictive value for the determination of cancer-free prostate quadrants could be increased from 70.6% to 91.1% in the anterior prostate and from 78.5% to 91.7% in the posterior prostate [59]. However, when using DW-MRI for lesion-targeting and procedure planning, it should be noted that ADC maps may underestimate the tumor volume in up to 50% of cases, especially in low-volume PCa [60].

DW-MRI as a tool for treatment response evaluation

With expanding individualization and diversification of management approaches to PCa, non-invasive imaging methods gain importance to monitor treatment response and ensure early detection of treatment failure. DW-MRI derived parameters have been described as potential markers of treatment response in several scenarios. Androgen-deprivation therapy was shown to increase the ADC of primary PCa lesions while decreasing the ADC of benign prostate tissue [61–63]. In metastatic PCa treated with androgen-deprivation, Reischauer and colleagues showed a significant increase of mean ADC of ^{99m}Tc-dicarboxypropane diphosphonate scintigraphy-detected pelvic bone metastases within one month [64]. This method could therefore allow for quantitative treatment response assessment in osteoblastic metastases, which are deemed non-measurable according to current response evaluation criteria (i.e. RECIST version 1.1) [65]. DW-MRI has also been used to assess and quantify tumor necrosis after targeted and photodynamic PCa therapy in animal models where the mean/median ADC of treated tumors significantly increased within 24–48 hours while it remained stable in control animals, respectively [66–67]. In another mouse model of metastatic prostate cancer, it was shown that cabozatinib-induced tumor necrosis was paralleled by an increase in mean tumor ADC [68]. In patients with treatment-naïve bone metastases (i.e. seven men with PCa and four women with breast cancer), Blackledge et al. used a semi-automatic segmentation algorithm for estimation of whole-body tumor burden and treatment response evaluation with DW-MRI [69]. Patients who responded to systemic treatment, as determined by imaging findings, tumor markers, and clinical parameters, showed a significantly larger increase in median global ADC than non-responders [54]. The change in whole-body tumor volume, as quantified by ‘tumor diffusion volume’, was significantly higher in non-responders than in responders (Figure 5) [69].

Others found that successful intensity-modulated radiotherapy increases the cancer's mean ADC early after initiation of therapy [70–72] and that post-radiation mean ADC-values may help to identify patients at risk for disease recurrence within 3 years (area under the ROC-curve: 0.88) [73]. In the field of laser interstitial thermal therapy, a preliminary study on five PCa patients reported that T2w-MRI-derived texture features and mean ADC values were most significant to detect and quantify therapy-induced changes [74].

Conclusion

As an integral part of multiparametric prostate MRI, DW-MRI improves the diagnostic performance in terms of tumor localization and local tumor staging. DW-MRI derived quantitative metrics, most importantly ADC, histogram analysis, diffusion kurtosis and texture features, can help to optimize pre-therapeutic risk assessment. These parameters can support and guide management decisions, most promising for the proper selection of patients for active surveillance programs. Finally, there is growing evidence for the use of DW-MRI in the assessment of treatment response of primary and metastatic PCa. A deeper understanding of the biologic and molecular basis of DW-MRI and the development of technical and analytic standards are currently the key challenges for translation of these novel applications into clinical routine.

References

1. Barentsz JO, Richenberg J, Clements R, Choyke P, Verma S, Villeirs G, Rouviere O, Logager V, Futterer JJ. ESUR prostate MR guidelines 2012. Eur Radiol. 2012; 22(4):746–757. [PubMed: 22322308]
2. Eberhardt SC, Carter S, Casalino DD, Merrick G, Frank SJ, Gottschalk AR, Leyendecker JR, Nguyen PL, Oto A, Porter C, Remer EM, Rosenthal SA. ACR Appropriateness Criteria prostate cancer--pretreatment detection, staging, and surveillance. J Am Coll Radiol. 2013; 10(2):83–92. [PubMed: 23374687]
3. Tan CH, Wei W, Johnson V, Kundra V. Diffusion-weighted MRI in the detection of prostate cancer: meta-analysis. AJR Am J Roentgenol. 2012; 199(4):822–829. [PubMed: 22997374]
4. Jie C, Rongbo L, Ping T. The value of diffusion-weighted imaging in the detection of prostate cancer: a meta-analysis. Eur Radiol. 2014; 24(8):1929–1941. [PubMed: 24865693]
5. Wu LM, Xu JR, Ye YQ, Lu Q, Hu JN. The clinical value of diffusion-weighted imaging in combination with T2-weighted imaging in diagnosing prostate carcinoma: a systematic review and meta-analysis. AJR Am J Roentgenol. 2012; 199(1):103–110. [PubMed: 22733900]
6. Tan CH, Hobbs BP, Wei W, Kundra V. Dynamic contrast-enhanced MRI for the detection of prostate cancer: meta-analysis. AJR Am J Roentgenol. 2015; 204(4):W439–448. [PubMed: 25794093]
7. Medved M, Soylu-Boy FN, Karademir I, Sethi I, Yousuf A, Karczmar GS, Oto A. High-resolution diffusion-weighted imaging of the prostate. AJR Am J Roentgenol. 2014; 203(1):85–90. [PubMed: 24951199]
8. Nguyen C, Sharif-Afshar AR, Fan Z, Xie Y, Wilson S, Bi X, Payor L, Saouaf R, Kim H, Li D. 3D high-resolution diffusion-weighted MRI at 3T: Preliminary application in prostate cancer patients undergoing active surveillance protocol for low-risk prostate cancer. Magn Reson Med. 2015; 11(10):25609.
9. Jahn JL, Giovannucci EL, Stampfer MJ. The high prevalence of undiagnosed prostate cancer at autopsy: implications for epidemiology and treatment of prostate cancer in the Prostate-specific Antigen-era. Int J Cancer. 2015; 137(12):2795–2802. [PubMed: 25557753]
10. NCI. [Accessed 2015/06/01] Surveillance, Epidemiology, and End Results Program. 2015. http://seer.cancer.gov/statfacts/html/prost.html

11. Epstein JI, Allsbrook WC Jr, Amin MB, Egevad LL. The 2005 International Society of Urological Pathology (ISUP) Consensus Conference on Gleason Grading of Prostatic Carcinoma. Am J Surg Pathol. 2005; 29(9):1228–1242. [PubMed: 16096414]
12. Pierorazio PM, Walsh PC, Partin AW, Epstein JI. Prognostic Gleason grade grouping: data based on the modified Gleason scoring system. BJU Int. 2013; 111(5):753–760. [PubMed: 23464824]
13. Cohen MS, Hanley RS, Kurteva T, Ruthazer R, Silverman ML, Sorcini A, Hamawy K, Roth RA, Tuerk I, Libertino JA. Comparing the Gleason prostate biopsy and Gleason prostatectomy grading system: the Lahey Clinic Medical Center experience and an international meta-analysis. Eur Urol. 2008; 54(2):371–381. [PubMed: 18395322]
14. Itou Y, Nakanishi K, Narumi Y, Nishizawa Y, Tsukuma H. Clinical utility of apparent diffusion coefficient (ADC) values in patients with prostate cancer: can ADC values contribute to assess the aggressiveness of prostate cancer? J Magn Reson Imaging. 2011; 33(1):167–172. [PubMed: 21182135]
15. Verma S, Rajesh A, Morales H, Lemen L, Bills G, Delworth M, Gaitonde K, Ying J, Samartunga R, Lamba M. Assessment of aggressiveness of prostate cancer: correlation of apparent diffusion coefficient with histologic grade after radical prostatectomy. AJR Am J Roentgenol. 2011; 196(2): 374–381. [PubMed: 21257890]
16. Hambrock T, Somford DM, Huisman HJ, van Oort IM, Witjes JA, Hulsbergen-van de Kaa CA, Scheenen T, Barentsz JO. Relationship between Apparent Diffusion Coefficients at 3.0-T MR Imaging and Gleason Grade in Peripheral Zone Prostate Cancer. Radiology. 2011; 14:14.
17. Vargas HA, Akin O, Franiel T, Mazaheri Y, Zheng J, Moskowitz C, Udo K, Eastham J, Hricak H. Diffusion-weighted endorectal MR imaging at 3 T for prostate cancer: tumor detection and assessment of aggressiveness. Radiology. 2011; 259(3):775–784. [PubMed: 21436085]
18. Hambrock T, Somford DM, Huisman HJ, van Oort IM, Witjes JA, Hulsbergen-van de Kaa CA, Scheenen T, Barentsz JO. Relationship between apparent diffusion coefficients at 3.0-T MR imaging and Gleason grade in peripheral zone prostate cancer. Radiology. 2011; 259(2):453–461. [PubMed: 21502392]
19. Bittencourt LK, Barentsz JO, de Miranda LC, Gasparetto EL. Prostate MRI: diffusion-weighted imaging at 1.5T correlates better with prostatectomy Gleason Grades than TRUS-guided biopsies in peripheral zone tumours. Eur Radiol. 2012; 22(2):468–475. [PubMed: 21913058]
20. Oto A, Yang C, Kayhan A, Tretiakova M, Antic T, Schmid-Tannwald C, Eggener S, Karczmar GS, Stadler WM. Diffusion-weighted and dynamic contrast-enhanced MRI of prostate cancer: correlation of quantitative MR parameters with Gleason score and tumor angiogenesis. AJR Am J Roentgenol. 2011; 197(6):1382–1390. [PubMed: 22109293]
21. Jung SI, Donati OF, Vargas HA, Goldman D, Hricak H, Akin O. Transition zone prostate cancer: incremental value of diffusion-weighted endorectal MR imaging in tumor detection and assessment of aggressiveness. Radiology. 2013; 269(2):493–503. [PubMed: 23878284]
22. Somford DM, Hambrock T, Hulsbergen-van de Kaa CA, Futterer JJ, van Oort IM, van Basten JP, Karthaus HF, Witjes JA, Barentsz JO. Initial experience with identifying high-grade prostate cancer using diffusion-weighted MR imaging (DWI) in patients with a Gleason score </= 3 + 3 = 6 upon schematic TRUS-guided biopsy: a radical prostatectomy correlated series. Invest Radiol. 2012; 47(3):153–158. [PubMed: 22293513]
23. Donati OF, Mazaheri Y, Afaq A, Vargas HA, Zheng J, Moskowitz CS, Hricak H, Akin O. Prostate cancer aggressiveness: assessment with whole-lesion histogram analysis of the apparent diffusion coefficient. Radiology. 2014; 271(1):143–152. [PubMed: 24475824]
24. Peng Y, Jiang Y, Antic T, Giger ML, Eggener SE, Oto A. Validation of quantitative analysis of multiparametric prostate MR images for prostate cancer detection and aggressiveness assessment: a cross-imager study. Radiology. 2014; 271(2):461–471. [PubMed: 24533870]
25. Borren A, Moman MR, Groenendaal G, Boeken Kruger AE, van Diest PJ, van der Groep P, van der Heide UA, van Vulpen M, Philippens ME. Why prostate tumour delineation based on apparent diffusion coefficient is challenging: an exploration of the tissue microanatomy. Acta Oncol. 2013; 52(8):1629–1636. [PubMed: 23621751]
26. Gibbs P, Liney GP, Pickles MD, Zelhof B, Rodrigues G, Turnbull LW. Correlation of ADC and T2 measurements with cell density in prostate cancer at 3.0 Tesla. Invest Radiol. 2009; 44(9):572–576. [PubMed: 19692841]

27. Bae H, Yoshida S, Matsuoka Y, Nakajima H, Ito E, Tanaka H, Oya M, Nakayama T, Takeshita H, Kijima T, Ishioka J, Numao N, Koga F, Saito K, Akashi T, Fujii Y, Kihara K. Apparent diffusion coefficient value as a biomarker reflecting morphological and biological features of prostate cancer. Int Urol Nephrol. 2014; 46(3):555–561. [PubMed: 24022845]
28. Sadinski M, Medved M, Karademir I, Wang S, Peng Y, Jiang Y, Sammet S, Karczmar G, Oto A. Short-term reproducibility of apparent diffusion coefficient estimated from diffusion-weighted MRI of the prostate. Abdom Imaging. 2015; 25:25.
29. Peng Y, Jiang Y, Antic T, Sethi I, Schmid-Tannwald C, Eggener S, Oto A. Apparent diffusion coefficient for prostate cancer imaging: impact of B values. AJR Am J Roentgenol. 2014; 202(3):W247–253. [PubMed: 24555621]
30. Thormer G, Otto J, Reiss-Zimmermann M, Seiwerts M, Moche M, Garnov N, Franz T, Do M, Stolzenburg JU, Horn LC, Kahn T, Busse H. Diagnostic value of ADC in patients with prostate cancer: influence of the choice of b values. Eur Radiol. 2012; 22(8):1820–1828. [PubMed: 22527373]
31. Mazaheri Y, Vargas HA, Nyman G, Shukla-Dave A, Akin O, Hricak H. Diffusion-weighted MRI of the prostate at 3.0 T: comparison of endorectal coil (ERC) MRI and phased-array coil (PAC) MRI-The impact of SNR on ADC measurement. Eur J Radiol. 2013; 82(10):e515–520. [PubMed: 23810189]
32. Wibmer A, Hricak H, Gondo T, Matsumoto K, Veeraraghavan H, Fehr D, Zheng J, Goldman D, Moskowitz C, Fine SW, Reuter VE, Eastham J, Sala E, Vargas HA. Haralick texture analysis of prostate MRI: utility for differentiating non-cancerous prostate from prostate cancer and differentiating prostate cancers with different Gleason scores. Eur Radiol. 2015; 21:21.
33. Rosenkrantz AB, Triolo MJ, Melamed J, Rusinek H, Taneja SS, Deng FM. Whole-lesion apparent diffusion coefficient metrics as a marker of percentage Gleason 4 component within Gleason 7 prostate cancer at radical prostatectomy. J Magn Reson Imaging. 2015; 41(3):708–714. [PubMed: 24616064]
34. Vargas HA, Lawrence EM, Mazaheri Y, Sala E. Updates in advanced diffusion-weighted magnetic resonance imaging techniques in the evaluation of prostate cancer. World J Radiol. 2015; 7(8): 184–188. [PubMed: 26339460]
35. Dopfert J, Lemke A, Weidner A, Schad LR. Investigation of prostate cancer using diffusion-weighted intravoxel incoherent motion imaging. Magnetic resonance imaging. 2011; 29(8):1053–1058. DOI: 10.1016/j.mri.2011.06.001 [PubMed: 21855241]
36. Shinmoto H, Tamura C, Soga S, Shiomi E, Yoshihara N, Kaji T, Mulkern RV. An intravoxel incoherent motion diffusion-weighted imaging study of prostate cancer. AJR American journal of roentgenology. 2012; 199(4):W496–500. DOI: 10.2214/ajr.11.8347 [PubMed: 22997399]
37. Zhang YD, Wang Q, Wu CJ, Wang XN, Zhang J, Liu H, Liu XS, Shi HB. The histogram analysis of diffusion-weighted intravoxel incoherent motion (IVIM) imaging for differentiating the gleason grade of prostate cancer. Eur Radiol. 2015; 25(4):994–1004. [PubMed: 25430007]
38. Steven AJ, Zhuo J, Melhem ER. Diffusion kurtosis imaging: an emerging technique for evaluating the microstructural environment of the brain. AJR Am J Roentgenol. 2014; 202(1):W26–33. [PubMed: 24370162]
39. Quentin M, Pentang G, Schimmoller L, Kott O, Muller-Lutz A, Blondin D, Arsov C, Hiester A, Rabenalt R, Wittsack HJ. Feasibility of diffusional kurtosis tensor imaging in prostate MRI for the assessment of prostate cancer: Preliminary results. Magnetic resonance imaging. 2014; 32(7):880–885. DOI: 10.1016/j.mri.2014.04.005 [PubMed: 24848289]
40. Rosenkrantz AB, Sigmund EE, Johnson G, Babb JS, Mussi TC, Melamed J, Taneja SS, Lee VS, Jensen JH. Prostate cancer: feasibility and preliminary experience of a diffusional kurtosis model for detection and assessment of aggressiveness of peripheral zone cancer. Radiology. 2012; 264(1): 126–135. DOI: 10.1148/radiol.12112290 [PubMed: 22550312]
41. Suo S, Chen X, Wu L, Zhang X, Yao Q, Fan Y, Wang H, Xu J. Non-Gaussian water diffusion kurtosis imaging of prostate cancer. Magnetic resonance imaging. 2014; 32(5):421–427. DOI: 10.1016/j.mri.2014.01.015 [PubMed: 24602826]
42. Wang Q, Li H, Yan X, Wu CJ, Liu XS, Shi HB, Zhang YD. Histogram analysis of diffusion kurtosis magnetic resonance imaging in differentiation of pathologic Gleason grade of prostate cancer. Urol Oncol. 2015; 33(8):337 e315–324.

43. Li C, Chen M, Li S, Zhao X, Zhang C, Luo X, Zhou C. Detection of prostate cancer in peripheral zone: comparison of MR diffusion tensor imaging, quantitative dynamic contrast-enhanced MRI, and the two techniques combined at 3.0 T. Acta radiologica (Stockholm, Sweden: 1987). 2014; 55(2):239–247. DOI: 10.1177/0284185113494978
44. Roethke MC, Kuder TA, Kuru TH, Fenchel M, Hadaschik BA, Laun FB, Schlemmer HP, Stieltjes B. Evaluation of Diffusion Kurtosis Imaging Versus Standard Diffusion Imaging for Detection and Grading of Peripheral Zone Prostate Cancer. Invest Radiol. 2015; 50(8):483–489. [PubMed: 25867657]
45. Rosenkrantz AB, Padhani AR, Chenevert TL, Koh DM, De Keyzer F, Taouli B, Le Bihan D. Body diffusion kurtosis imaging: Basic principles, applications, and considerations for clinical practice. J Magn Reson Imaging. 2015; 42(5):1190–1202. [PubMed: 26119267]
46. Hambrock T, Hoeks C, Hulsbergen-van de Kaa C, Scheenen T, Futterer J, Bouwense S, van Oort I, Schroder F, Huisman H, Barentsz J. Prospective assessment of prostate cancer aggressiveness using 3-T diffusion-weighted magnetic resonance imaging-guided biopsies versus a systematic 10-core transrectal ultrasound prostate biopsy cohort. Eur Urol. 2012; 61(1):177–184. [PubMed: 21924545]
47. Zhang J, Xiu J, Dong Y, Wang M, Han X, Qin Y, Huang Z, Cai S, Yuan X, Liu Q. Magnetic resonance imagingdirected biopsy improves the prediction of prostate cancer aggressiveness compared with a 12core transrectal ultrasoundguided prostate biopsy. Mol Med Rep. 2014; 9(5): 1989–1997. [PubMed: 24584266]
48. Somford DM, Hoeks CM, Hulsbergen-van de Kaa CA, Hambrock T, Futterer JJ, Witjes JA, Bangma CH, Vergunst H, Smits GA, Oddens JR, van Oort IM, Barentsz JO. Evaluation of diffusion-weighted MR imaging at inclusion in an active surveillance protocol for low-risk prostate cancer. Invest Radiol. 2013; 48(3):152–157. [PubMed: 23328910]
49. Mitsuzuka K, Koga H, Sugimoto M, Arai Y, Ohyama C, Kakehi Y, Naito S. Current use of active surveillance for localized prostate cancer: A nationwide survey in Japan. Int J Urol. 2015; 10(10): 12813.
50. Preston MA, Feldman AS, Coen JJ, McDougal WS, Smith MR, Paly JJ, Carrasquillo R, Wu CL, Dahl DM, Barrisford GW, Blute ML, Zietman AI. Active surveillance for low-risk prostate cancer: Need for intervention and survival at 10 years. Urol Oncol. 2015; 6(15):00194–00195.
51. van As NJ, de Souza NM, Riches SF, Morgan VA, Sohaib SA, Dearnaley DP, Parker CC. A study of diffusion-weighted magnetic resonance imaging in men with untreated localised prostate cancer on active surveillance. Eur Urol. 2009; 56(6):981–987. [PubMed: 19095345]
52. Giles SL, Morgan VA, Riches SF, Thomas K, Parker C, deSouza NM. Apparent diffusion coefficient as a predictive biomarker of prostate cancer progression: value of fast and slow diffusion components. AJR Am J Roentgenol. 2011; 196(3):586–591. [PubMed: 21343500]
53. Flavell RR, Westphalen AC, Liang C, Sotto CC, Noworolski SM, Vigneron DB, Wang ZJ, Kurhanewicz J. Abnormal findings on multiparametric prostate magnetic resonance imaging predict subsequent biopsy upgrade in patients with low risk prostate cancer managed with active surveillance. Abdom Imaging. 2014; 39(5):1027–1035. [PubMed: 24740760]
54. Jeong CW, Park YH, Hwang SI, Lee S, Jeong SJ, Hong SK, Byun SS, Lee HJ, Lee SE. The role of 3-tesla diffusion-weighted magnetic resonance imaging in selecting prostate cancer patients for active surveillance. Prostate Int. 2014; 2(4):169–175. [PubMed: 25599072]
55. Morgan VA, Riches SF, Thomas K, Vanas N, Parker C, Giles S, Desouza NM. Diffusion-weighted magnetic resonance imaging for monitoring prostate cancer progression in patients managed by active surveillance. Br J Radiol. 2011; 84(997):31–37. [PubMed: 21172965]
56. Lee DH, Koo KC, Lee SH, Rha KH, Choi YD, Hong SJ, Chung BH. Tumor lesion diameter on diffusion weighted magnetic resonance imaging could help predict insignificant prostate cancer in patients eligible for active surveillance: preliminary analysis. J Urol. 2013; 190(4):1213–1217. [PubMed: 23727188]
57. Rosenkrantz AB, Prabhu V, Sigmund EE, Babb JS, Deng FM, Taneja SS. Utility of diffusional kurtosis imaging as a marker of adverse pathologic outcomes among prostate cancer active surveillance candidates undergoing radical prostatectomy. AJR Am J Roentgenol. 2013; 201(4): 840–846. [PubMed: 24059373]

58. Park SY, Kim CK, Park BK, Lee HM, Lee KS. Prediction of biochemical recurrence following radical prostatectomy in men with prostate cancer by diffusion-weighted magnetic resonance imaging: initial results. Eur Radiol. 2011; 21(5):1111–1118. [PubMed: 21046403]
59. Matsuoka Y, Numao N, Saito K, Tanaka H, Kumagai J, Yoshida S, Ishioka J, Koga F, Masuda H, Kawakami S, Fujii Y, Kihara K. Candidate selection for quadrant-based focal ablation through a combination of diffusion-weighted magnetic resonance imaging and prostate biopsy. BJU Int. 2014; 14(10):12901.
60. Cornud F, Khoury G, Bouazza N, Beuvon F, Peyromaure M, Flam T, Zerbib M, Legmann P, Delongchamps NB. Tumor target volume for focal therapy of prostate cancer-does multiparametric magnetic resonance imaging allow for a reliable estimation? J Urol. 2014; 191(5):1272–1279. [PubMed: 24333516]
61. Nemoto K, Tateishi T, Ishidate T. Changes in diffusion-weighted images for visualizing prostate cancer during antiandrogen therapy: preliminary results. Urol Int. 2010; 85(4):421–426. [PubMed: 21051871]
62. Kim AY, Kim CK, Park SY, Park BK. Diffusion-weighted imaging to evaluate for changes from androgen deprivation therapy in prostate cancer. AJR Am J Roentgenol. 2014; 203(6):W645–650. [PubMed: 25415730]
63. Hotker AM, Mazaheri Y, Zheng J, Moskowitz CS, Berkowitz J, Lantos JE, Pei X, Zelefsky MJ, Hricak H, Akin O. Prostate Cancer: assessing the effects of androgen-deprivation therapy using quantitative diffusion-weighted and dynamic contrast-enhanced MRI. Eur Radiol. 2015; 29:29.
64. Reischauer C, Froehlich JM, Koh DM, Graf N, Padevit C, John H, Binkert CA, Boesiger P, Gutzeit A. Bone metastases from prostate cancer: assessing treatment response by using diffusion-weighted imaging and functional diffusion maps--initial observations. Radiology. 2010; 257(2): 523–531. [PubMed: 20829534]
65. Eisenhauer EA, Therasse P, Bogaerts J, Schwartz LH, Sargent D, Ford R, Dancey J, Arbuck S, Gwyther S, Mooney M, Rubinstein L, Shankar L, Dodd L, Kaplan R, Lacombe D, Verweij J. New response evaluation criteria in solid tumours: revised RECIST guideline (version 1.1). Eur J Cancer. 2009; 45(2):228–247. [PubMed: 19097774]
66. Baker LC, Boult JK, Walker-Samuel S, Chung YL, Jamin Y, Ashcroft M, Robinson SP. The HIF-pathway inhibitor NSC-134754 induces metabolic changes and anti-tumour activity while maintaining vascular function. Br J Cancer. 2012; 106(10):1638–1647. [PubMed: 22498643]
67. Wang H, Fei B. Diffusion-weighted MRI for monitoring tumor response to photodynamic therapy. J Magn Reson Imaging. 2010; 32(2):409–417. [PubMed: 20677270]
68. Graham TJ, Box G, Tunariu N, Crespo M, Spinks TJ, Miranda S, Attard G, de Bono J, Eccles SA, Davies FE, Robinson SP. Preclinical evaluation of imaging biomarkers for prostate cancer bone metastasis and response to cabozantinib. J Natl Cancer Inst. 2014; 106(4):dju033. [PubMed: 24634505]
69. Blackledge MD, Collins DJ, Tunariu N, Orton MR, Padhani AR, Leach MO, Koh DM. Assessment of treatment response by total tumor volume and global apparent diffusion coefficient using diffusion-weighted MRI in patients with metastatic bone disease: a feasibility study. PLoS One. 2014; 9(4):e91779. [PubMed: 24710083]
70. Park SY, Kim CK, Park BK, Park W, Park HC, Han DH, Kim B. Early changes in apparent diffusion coefficient from diffusion-weighted MR imaging during radiotherapy for prostate cancer. Int J Radiat Oncol Biol Phys. 2012; 83(2):749–755. [PubMed: 22154286]
71. Decker G, Murtz P, Gieseke J, Traber F, Block W, Sprinkart AM, Leitzen C, Buchstab T, Lutter C, Schuller H, Schild HH, Willinek WA. Intensity-modulated radiotherapy of the prostate: dynamic ADC monitoring by DWI at 3.0 T. Radiother Oncol. 2014; 113(1):115–120. [PubMed: 25304719]
72. Song I, Kim CK, Park BK, Park W. Assessment of response to radiotherapy for prostate cancer: value of diffusion-weighted MRI at 3 T. AJR Am J Roentgenol. 2010; 194(6):W477–482. [PubMed: 20489065]
73. Liu L, Wu N, Ouyang H, Dai JR, Wang WH. Diffusion-weighted MRI in early assessment of tumour response to radiotherapy in high-risk prostate cancer. Br J Radiol. 2014; 87(1043): 20140359. [PubMed: 25162831]

74. Viswanath S, Toth R, Rusu M, Sperling D, Lepor H, Futterer J, Madabhushi A. Quantitative Evaluation of Treatment Related Changes on Multi-Parametric MRI after Laser Interstitial Thermal Therapy of Prostate Cancer. Proc SPIE Int Soc Opt Eng. 2013; 8671:86711F.

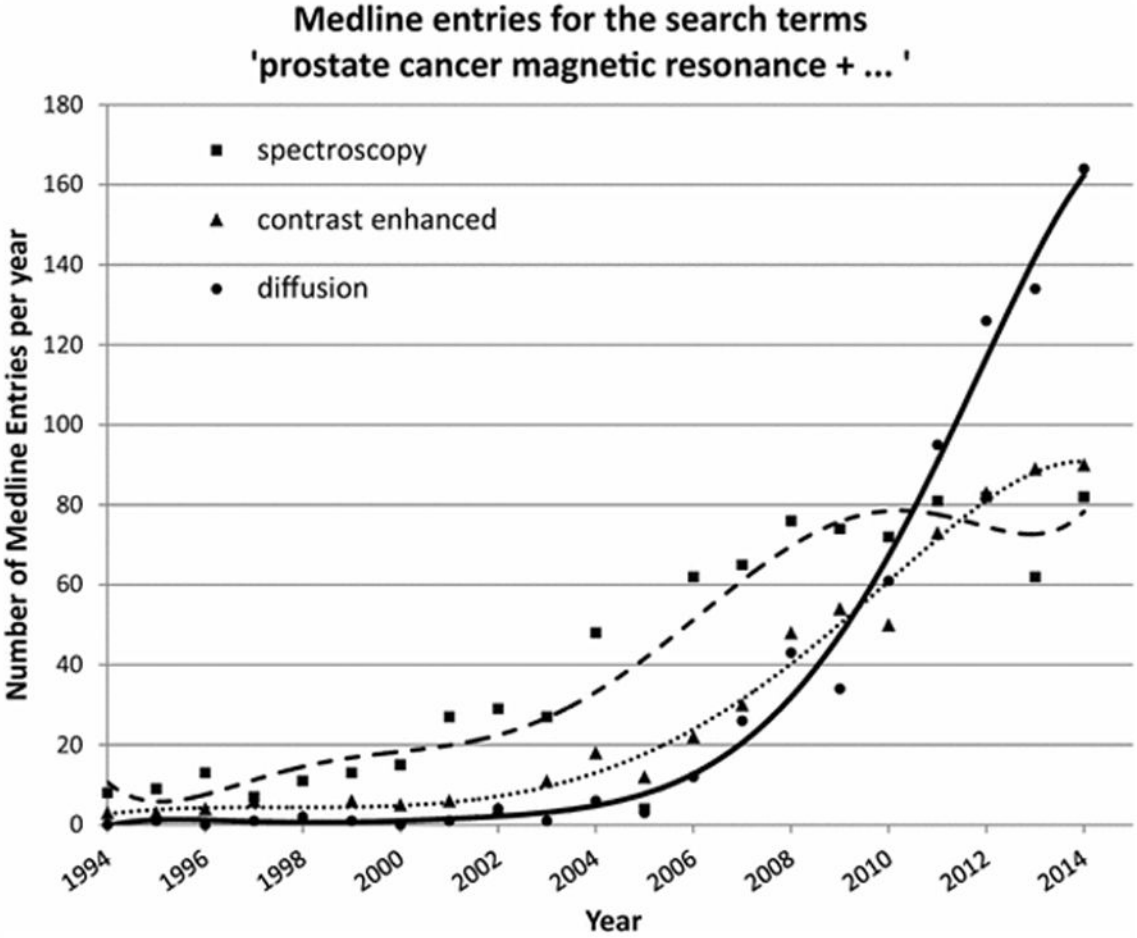

Figure 1.

Number of annual Medline Entries for the search terms ‘prostate cancer magnetic resonance + SPECTROSCOPY’ (squares, dashed line), ‘prostate cancer magnetic resonance + CONTRAST ENHANCED’ (triangles, dotted line), and ‘prostate cancer magnetic resonance + DIFFUSION’ (circles, solid line).

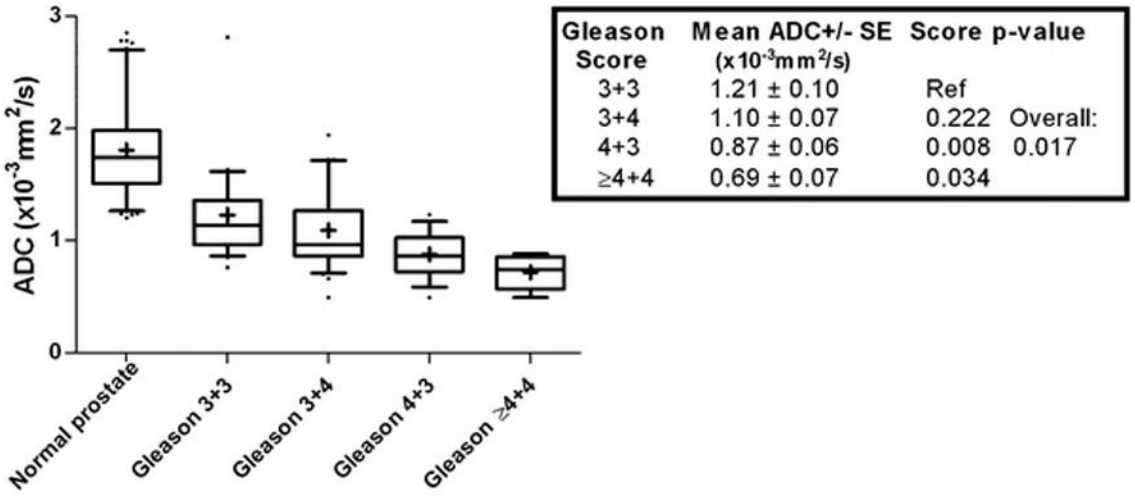

Figure 2.

Box and whisker plots showing the mean ADC of normal prostate tissue and prostate cancer lesions stratified by Gleason score from [17]. This graph illustrates the significant correlation of ADC and Gleason score but also highlights the substantial overlap between the categories. For example, a given cancer with a mean ADC of $0.9\times10^{-3}mm^2/s$ could fall into different categories. As a consequence, there are no clear ADC cut-off values to differentiate low- from high grade tumors.

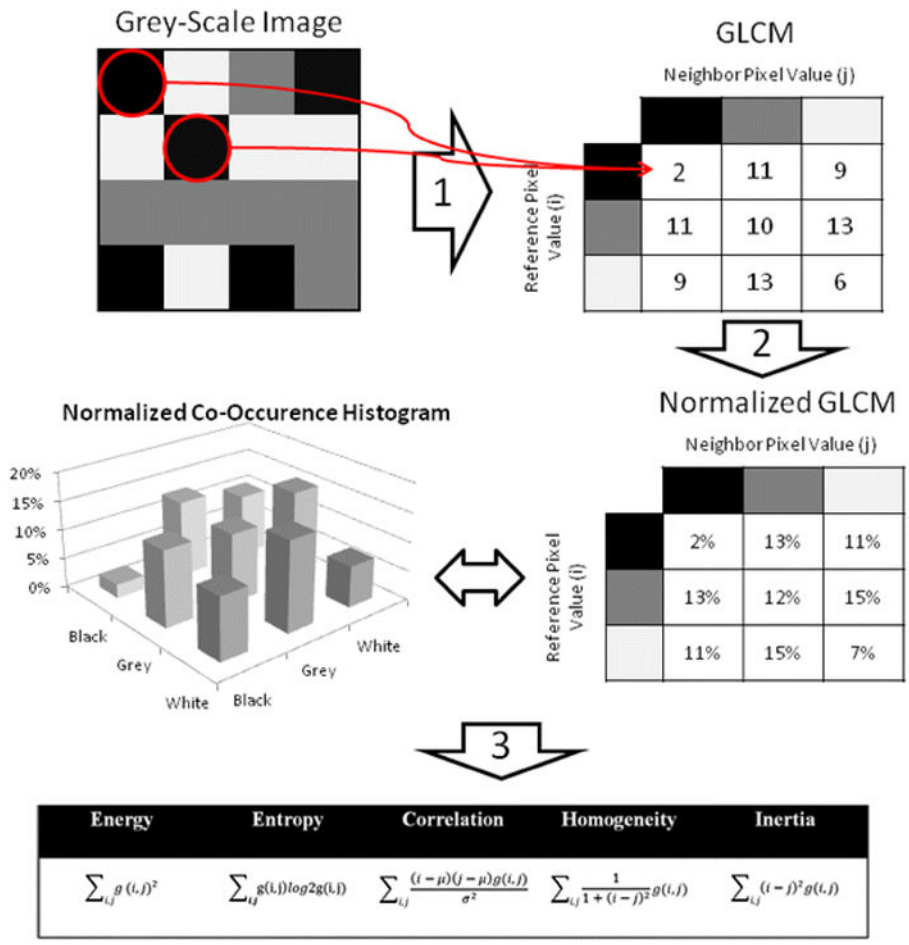

Figure 3.

Example for the calculation of texture features from a grey-level co-occurrence matrix (GLCM). For the sake of simplicity, a 4 × 4 pixel grey-scale image with only three grey-levels (i.e. white, grey, and black) was chosen. In Step 1, a GLCM is deducted from this image by considering the relationship of every pixel to its neighborhood. We start with the co-occurrence of ‘black + black’, which occurs twice in the image, as indicated by the red circles. The absolute count of the different co-occurrences is recorded in a table, which - after its completion - is named the GLCM. In Step 2, the GLCM is normalized so that each cell doesn’t contain a count but the probability of every possible co-occurrence. These probabilities provide the basis for the calculation of the various ‘texture features’ according to the equations shown (Step 3).

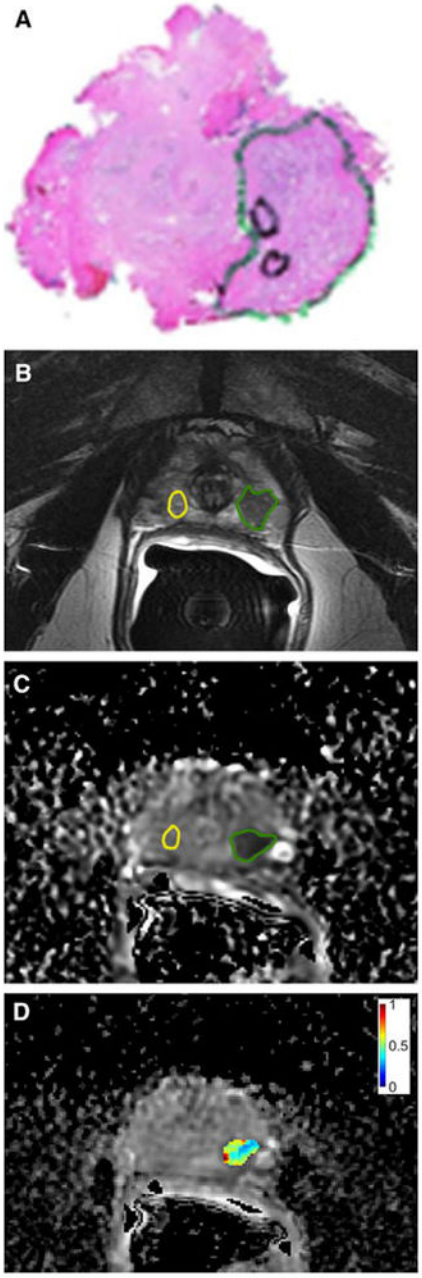

Figure 4.

Whole-mount prostatectomy histopathology specimen (a), multiparametric prostate MRI (b,c) with texture analysis (d) of a 63-year-old man. **(a)** Whole-mount histopathology demonstrated a Gleason 3+4 prostate cancer (green circle). **(b)** T2-weighted imaging showed a corresponding region of low signal intensity in the peripheral zone (green circle) as compared to non-cancerous tissue (yellow circle). **(c)** The cancer showed restricted diffusion on the apparent diffusion coefficient (ADC) map (green circle). (d) Texture analysis of the ADC map showing the normalized ADC Entropy map of the tumour. Reprinted with permission from [32].

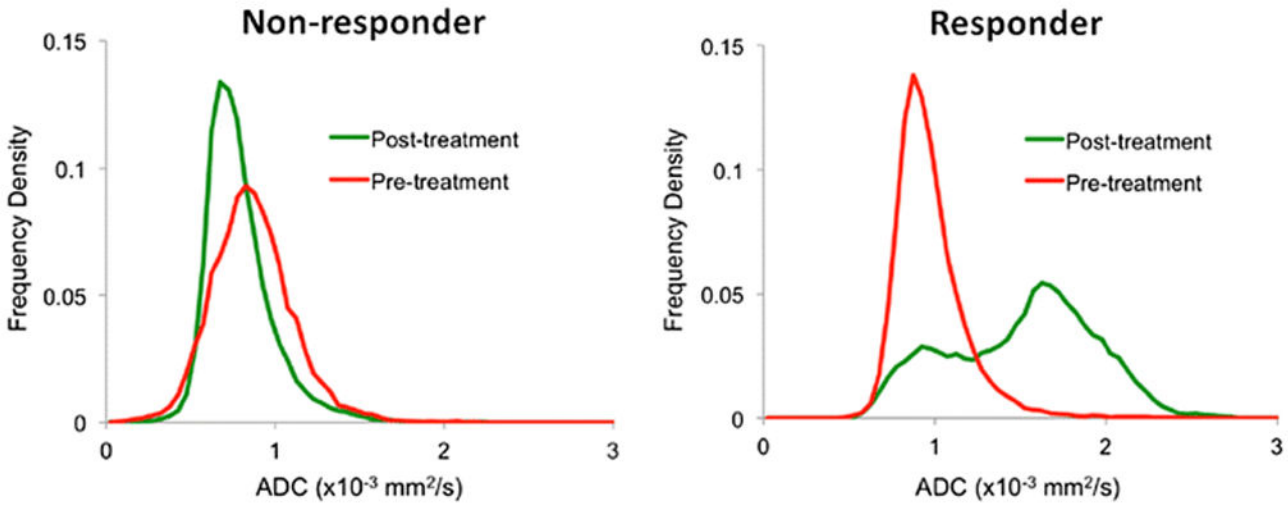

Figure 5.

Pre- and post-treatment ADC-value distributions derived from whole-body DW-MRI of patients undergoing chemotherapy for metastasized prostate cancer from [69]. In contrast to a non-responder (left diagram), the authors observed a clear shift of the histogram distribution towards higher ADC values in a responder (right diagram).